Cold Regions Science and Technology 194 (2022) 103456

Contents lists available at ScienceDirect

Cold Regions Science and Technology

journal homepage: www.elsevier.com/locate/coldregions

The influence of soil texture and environmental conditions on frozen soil infiltration: A numerical investigation

Joris C. Stuurop [a,*], Sjoerd E.A.T.M. van der Zee [b,c], Helen K. French [a]

[a] Faculty of Environmental Sciences and Natural Resource Management, Norwegian University of Life Sciences, Høgskoleveien 12, 1433 Ås, Norway
[b] Department of Environmental Sciences, Wageningen University & Research, Droevendaalsesteeg 3, 6708 PB Wageningen, the Netherlands
[c] School of Chemistry, Monash University, Melbourne, VIC 3800, Australia

ARTICLE INFO

Keywords:
Frozen soil
Modelling
Infiltration
Cold regions
Unsaturated zone
Cryosphere

ABSTRACT

Frozen soil increases overland flow and flood risk, but the question remains under which conditions frozen soil significantly impedes infiltration. In this study, we simulated infiltration into frozen soil with a numerical model to investigate theoretical controls on frozen soil infiltration for several soil types. We found that the infiltration capacities of soils with intermediate texture are most significantly affected by freezing. Furthermore, we examined the influence of initial saturation, boundary temperature conditions and water input rate and found non-linear relationships with frozen soil infiltration. Freezing of infiltrated water particularly impeded infiltration. Two different temporal frozen soil infiltration regimes were detected. This study could help identify situations in which the impact of freezing on catchment hydrology is expected to be large. It also provides a starting point for further experimental work.

1. Introduction

At northern latitudes and high altitudes, the soil often freezes and thaws seasonally. In addition, water is stored as snow over the winter and released into the environment again during snowmelt in spring. The combination of high water input during snowmelt and still frozen soil is associated with flood and erosion risk, because frozen soil has a reduced hydraulic conductivity (Rango and DeWalle, 2008; Ireson et al., 2013). The altered pathway of melt- and rainwater due to frozen soil also affects the fate of contaminants in the landscape (French et al., 2002). Other consequences of frozen soil include focused infiltration and erosion of fertile topsoil (French and Binley, 2004; Hayashi, 2013). Despite these observed consequences of frozen soil in several studies, it is still unclear when soil frost will have a significant impact on water partitioning at the catchment scale (Ala-Aho et al., 2021). Some studies for example show frozen soil to have no significant impact on streamflow (Granger et al., 1984; Nyberg et al., 2001; Stähli, 2017), while in other studies the impact was significant (Blackburn et al., 1990; Jones and Pomeroy, 2001; Coles and McDonnell, 2018). More insight is therefore needed into the factors that determine frozen soil infiltration capacity.

A popular categorization of infiltration capacity of frozen soil has been formulated by Gray and Granger (1986) based on field experiments. They determined the following categories: 1) restricted infiltration: infiltration volumes are negligible due to concrete frost; 2) limited infiltration: infiltration occurs but is reduced due to a degree of ice saturation; and 3) unlimited infiltration: macropores and fractures allow all water to infiltrate. This categorization, however, obscures detail about infiltration into frozen soil since infiltration is likely to occur along a gradient from unlimited to fully restricted depending on numerous factors such as ice content, soil temperature and soil texture. It has been found that higher ice saturation, and therefore higher initial saturation before freezing, decreases frozen soil infiltration capacity (McCauley et al., 2002; Hayashi, 2013). Further details on the effects of the environmental conditions on different soil types, such the shape of the relationship between initial saturation and eventual frozen soil infiltration, are lacking.

Several processes occur simultaneously in a freezing soil, such as the phase change of water with associated latent heat flux, capillary and gravitational flow, conduction of heat through the solid and liquid soil constituents, and cryosuction - the increase in matric potential of (partly) frozen soil volumes resulting in redistribution of unfrozen water (Ireson et al., 2013). Given the complex interactions of these processes, it is hard to predict how soil properties and environmental parameters (e.g., air temperature and initial soil moisture state) affect frozen soil

* Corresponding author.
E-mail addresses: joris.stuurop@nmbu.no (J.C. Stuurop), sjoerd.vanderzee@wur.nl (S.E.A.T.M. van der Zee), helen.french@nmbu.no (H.K. French).

https://doi.org/10.1016/j.coldregions.2021.103456
Received 1 April 2021; Received in revised form 24 November 2021; Accepted 29 November 2021
Available online 8 December 2021

infiltration capacity. Laboratory and field testing would be demanding in view of the many possible values of process parameters, further complicated by the difficulty of measuring ice and unfrozen water content in soils (Azmatch et al., 2012). The gain of most experimental studies is therefore mostly qualitative rather than quantitative understanding, despite providing useful measurements and insights (Stähli et al., 1999).

Regarding the temporal pattern of infiltration into frozen soil, Watanabe et al. (2012) observed three phases of frozen soil infiltration in their soil column experiment: (1) no infiltration due to in-situ freezing of infiltrating water, followed by (2) slow infiltration as water moves through the slowly thawing frozen zone and then (3) normal infiltration due to the progression of significant thaw. Zhao and Gray (1998) also proposed that infiltration rate changes with time, but quite differently: first, a short transient phase (several hours) when infiltration and heat transfer rate decrease rapidly, followed by a quasi-steady-state regime when changes in infiltration and heat transfer rate are small. These different results of Watanabe et al. (2012) and Zhao and Gray (1998) indicate that the temporal infiltration regime itself is likely dependent on soil type and environmental conditions.

Numerical simulation provides an opportunity to test a large number of soil parameters and environmental conditions in relation to frozen soil infiltration. It can help predict the response to freezing of different soil texture classes during different temperature and moisture conditions. The numerical calculations could also reveal possible hydrological threshold values at which freezing starts to have a significant effect on infiltration. While several numerical models have been created to simulate water and heat transport in variably-saturated frozen soils (Kurylyk and Watanabe, 2013), few models have been used to quantitatively explore the effect of various soil and environmental parameters on frozen soil infiltration capacity.

The study of thaw and infiltration into frozen soil with physically based numerical models, i.e., the end of winter and beginning of spring period, has received attention in the studies by Larsbo et al. (2019) and Mohammed et al. (2021). Numerical experiments with the dual-permeability model of Larsbo et al. (2019) found that percolation at the bottom of the soil column is dominated by preferential flow through macropores in a macroporous soil because the hydraulic conductivity of the micropore domain is reduced by ice. They also show that depending on energy transfer rate, macropores can be blocked by ice due to freezing of infiltrated water. Mohammed et al. (2021) reached a similar conclusion as their modelling study demonstrates that freezing of infiltrated water along preferential flowpaths severely reduce infiltration.

In this study, we use an existing single-domain numerical code to simulate the freezing and thawing of variably-saturated frozen soil columns in combination with infiltration of melt- and rainwater. First, we assessed whether the numerical code, which has previously been tested on freezing soil column experiments (Stuurop et al., 2021), could satisfactorily reproduce the full freeze-thaw temperature cycle of a laboratory soil column experiment as well as the infiltration pattern into a frozen soil. Subsequently, we performed a series of numerical 1D test simulations to investigate controlling factors on infiltration capacity of frozen soil, such as initial saturation, temperature boundary conditions and soil parameters. The results gave insight into the theoretical link between soil freezing and infiltration reduction, and the role soil and environmental parameters play herein. The focus lies on the soil matrix flow with a texture ranging from coarse to very fine are examined and environmental conditions are chosen to encompass a wide range of possible field situations.

2. Methods

2.1. Numerical model

In this study we employed the semi-empirical version of a numerical model that is described in detail by Stuurop et al. (2021). It is a one-dimensional water and heat transport model that includes phase changes between water and ice. We chose the semi-empirical version as it requires the least amount of parameters to simulate freezing. The energy exchange boundary between the soil and snow or atmosphere was simplified by a fixed temperature boundary at the top. Water flow was based on the Richards Equation for unsaturated flow (Richards, 1931), while heat transport was governed by the energy balance equation that includes thermal conduction, advection and latent heat transfer:

$$\frac{\partial T}{\partial t}\left[\theta_{uf}\rho_w H_w + \theta_i\rho_i H_i + \theta_a\rho_a H_a + (1-\varepsilon)\rho_s H_s\right] + \left[(H_i - H_w)T - \Delta L_f\right]\left[\left(\rho_i\frac{\partial\theta_i}{\partial T}\right)\frac{\partial T}{\partial t}\right] = -\frac{\partial T}{\partial z}\left(\theta_{uf}H_w\rho_w v\right) + \frac{\partial}{\partial z}\left(\overline{c}\,\frac{\partial T}{\partial z}\right) \quad (1)$$

where ρ_w is the density of water (kgm^{-3}), H_w is the specific heat of water (Jkg^{-1} K^{-1}), ρ_i is the density of ice (kgm^{-3}), H_i is the specific heat of ice (Jkg^{-1} K^{-1}), θ_a is the volumetric air content, ρ_a is the density of air (kgm^{-3}), H_a is the specific heat of air (Jkg^{-1} K^{-1}), ε is porosity, ρ_s is the density of solid soil (kgm^{-3}), H_s is the specific heat of solid soil (Jkg^{-1} K^{-1}), $\overline{c}$ is the thermal conductivity of the soil (Wm^{-1} K^{-1}), v is the flow velocity of unfrozen water (ms^{-1}), L_f is the latent heat of fusion (Jkg^{-1}) and z is the elevation (m).

The thermal conductivity was calculated as the geometric mean of the sum of thermal conductivities of all soil constituents (water, ice, air and solid grains). The van Genuchten model (van Genuchten, 1980) was used to calculate soil water retention. The increase in matric pressure due to freezing, i.e., cryosuction, was simulated through an empirical equation developed by Zhang et al. (2007) and Kulik (1978):

$$\psi = \psi_{vgn}{}^{*}(1 + C_k\theta_{ice})^2 \quad (2)$$

where ψ (m) is the matric potential of the soil (including the increase of matric potential due to ice content), ψ_{vgn} (m) is the matric potential of the soil based on the van Genuchten soil parameters for soil water retention (excluding the effect of ice content), and C_k is an empirical factor that represents the effect of ice on matric pressure.

The Clausius-Clapeyron relationship was incorporated into the van Genuchten equation to relate the unfrozen water content of the soil to the soil temperature:

$$\theta_{uf} = \theta_{res} + (\theta_{sat} - \theta_{res})\left[1 + \left(a_{vg}L_f\rho_w ln\frac{T + 273.15}{T_0 + 273.15}\right)^{n_{vg}}\right]^{-m_{vg}} \quad (3)$$

where θ_{uf} is the unfrozen water content, θ_{res} is the residual total water content, θ_{sat} is the saturated total water content, ρ_w is the density of water (kgm^{-3}), T is the temperature (°C), T_0 the freezing point of water (0 °C) and a_{vg}, n_{vg} and m_{vg} are model parameters.

Hydraulic conductivity was related to unfrozen water content through the following relationship, which is based on Mualem (1976) and van Genuchten (1980):

$$K = K_{sat}\left(\frac{\theta_{sat} - \theta_{res}}{\theta_{uf} - \theta_{res}}\right)^{0.5}\left\{1 - \left[1 - \left(\frac{\theta_{sat} - \theta_{res}}{\theta_{uf} - \theta_{res}}\right)^{\left(\frac{n-1}{n}\right)}\right]^{\left(\frac{n-1}{n}\right)}\right\}^2 \quad (4)$$

Table 1
Original soil properties measured in the frozen soil infiltration experiment by Pittman et al. (2020).

Soil layer	Bulk density (gcm^{-3})	Porosity	Ksat (ms^{-1})	Particle size percentage (sand-silt-clay)
Top	1.09	0.6	5.56e-06	9–62-29
Middle	1.38	0.51	1.97e-08	11–64-26
Bottom	1.44	0.51	1.16e-10	13–70-17

where K is the hydraulic conductivity of the soil (ms^{-1}; frozen or unfrozen) and K_{sat} is the saturated hydraulic conductivity (ms^{-1}). The effect of temperature on hydraulic conductivity by affecting the viscosity and density of water was neglected.

2.2. Experimental validation

The numerical model had previously been tested on three experimental datasets of freezing soil columns (Stuurop et al., 2021). To test the ability of the model to simulate the thermodynamic thawing process as well, we compared the results of the model to a full freeze-thaw cycle experiment by Wang et al. (2017) in which soil temperature was measured at different depths. In the experiment, a 20 cm column with silt soil at an initial temperature of 1 °C was periodically frozen and thawed from the top. The side walls were insulated, while the bottom temperature was kept at a constant temperature of 1 °C. Freezing and thawing periods each lasted 24 h, with temperatures of −5 and + 5 °C imposed on top of the soil column. This was repeated until a total of 6 days. The grain size fractions of the soil were reported in the original study, but not the water retention parameters and hydraulic conductivity. We therefore used the Rosetta pedo-transfer function (Rosetta Lite version 1.1) of the software program Hydrus-1D (Šimůnek et al., 1998) to estimate the soil water retention parameters for the van Genuchten model ($a = 0.021\ cm^{-1}$, $n = 1.3475$ and residual water content = 0.01), the saturated hydraulic conductivity (1.1e-06 ms^{-1}) and porosity (0.4) based on the grain size fractions. In the original experiment, frost heave occurred, a process which is not simulated by the numerical model. A discrepancy could therefore be expected after repeated freeze-thaw cycles as initial soil properties could be changed. Thermal conductivity of solid soil particles was calibrated to 1.5 $W\ mK^{-1}$.

A second dataset (Pittman et al., 2020) was used to test the capability of the model to simulate the physics of infiltration into frozen soil. This provides experimental data of infiltration into frozen repacked soil columns. A few difficulties hamper a direct translation from experimental conditions to the model setup however. Soil water retention parameters are unknown. Therefore, these parameters were initially estimated with the Rosetta pedotransfer function from the reported bulk density and grain size fractions. Since repacking of the soil occurred after these soil properties were measured, we further adjusted the water retention parameters based on the unfrozen water content at a certain subzero temperature via the soil freezing curve (SFC) equation. For the same reason, we calibrated the saturated hydraulic conductivity of the topsoil layer as it was measured prior to repacking when the soil still contained macropores. Furthermore, the vertical distribution of the three soil layers of the soil column had to be estimated. The model was made to have only two soil layers for simplification because most relevant water dynamics occurred in the topsoil and the SFC suggested little difference between the middle and bottom layer.

In the experiment, a heat lamp was used to warm up the soil with 250 Wm^{-2}. Given the 10 cm water column on top of the soil during the infiltration experiment, it is unclear how much of this energy is absorbed by the top of the soil. Therefore, the amount of energy added to the top boundary was manually calibrated to roughly match the resulting topsoil temperature recorded in the experiment. This gave temporally varying energy transfer to the soil between 50 and 150 Wm^{-2} due to the infiltration of the water column. Solid grain thermal conductivity was manually calibrated to 1 $Wm^{-1}\ K^{-1}$ to fit the temperature change rate. During the experiment, heat was added to the bottom of the soil column at an unknown timepoint and it is unclear how much energy this entails; we therefore ignored this since the main interest lies with the topsoil and we accept some discrepancy at the end of the experiment. Calibrated and estimated soil properties are later given in the Results section, Table 4. The original measurements of soil properties in the experiment are given in Table 1.

2.3. Sensitivity testing of the model

2.3.1. Setup

For the main goal of this study, we simulated a 50 cm deep soil column (soil textures and parameters defined in Table 3) exposed to varying temperatures and water input rates at the top boundary (Table 4), while the bottom boundary enabled free gravitational drainage. Water that does not infiltrate is removed from the surface and counted as non-infiltrated water, representing surface runoff in a hillslope situation (i.e., no ponding of water). The soil initially had a uniform temperature of 1 °C and uniform total water saturation. The first phase was a freezing period lasting 120 h, representing various situations that occur during a natural freezing period before snow cover. During this period, a constant top boundary freezing temperature was

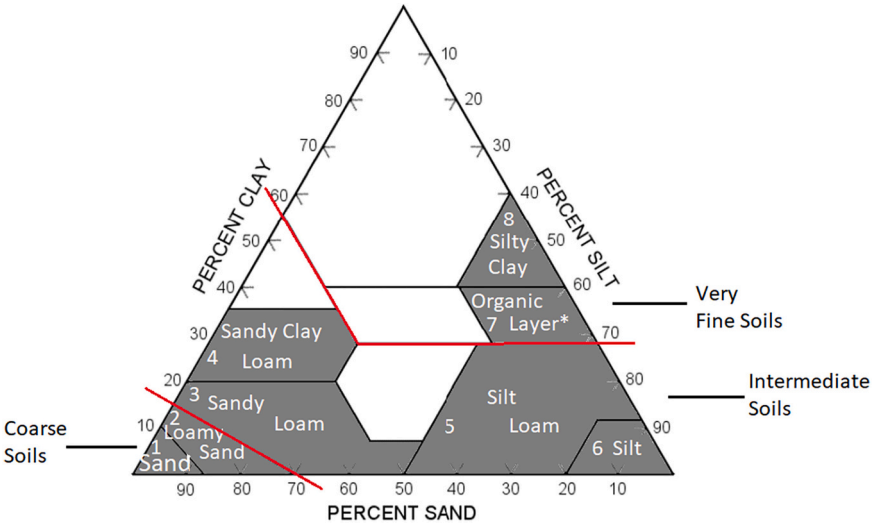

Fig. 1. Soil texture classification triangle. The dark gray areas are the soils simulated in this study, with the numbers referring to the soil numbers in Table 1. The large red lines distinguish between coarse, intermediate and very fine soils. The organic layer is placed in the area commonly classified as silty clay loam, because the organic layer has very similar water retention capacity compared to this soil type. (For interpretation of the references to colour in this figure legend, the reader is referred to the web version of this article.)

Table 2
Soil parameters used in the different simulations.

Soil nr.	Soil type	Ksat (ms^{-1})	a (cm^{-1})	n	Porosity	Sres
1	Sand	3.3e-04	0.074	2.96	0.33	0.03
2	Loamy Sand	4.05e-05	0.124	2.28	0.41	0.057
3	Sandy Loam	1.23e-05	0.075	1.89	0.41	0.065
4	Sandy Clay Loam	3.63e-06	0.059	1.48	0.39	0.1
5	Silt Loam	1.25e-06	0.02	1.41	0.45	0.067
6	Silt	6.94e-07	0.016	1.37	0.46	0.034
7	Organic Layer	9.26e-07	0.013	1.20	0.766	0.01
8	Silty Clay	5.56e-08	0.005	1.09	0.36	0.07

The values are based on soil cataloguing by Carsel and Parrish (1988). Ksat is the saturated hydraulic conductivity, a and n are van Genuchten soil water retention parameters and Sres is the residual water content.

varied (−0.25 to −4 °C) resulting in different levels of ice saturation. In addition, we varied the initial saturation (0.25 to 1) to represent different antecedent moisture conditions.

The freezing phase was followed by a thawing and water infiltration phase of varying time length. The thawing temperatures (0 to 4 °C) represent different energy exchange conditions between the soil and the snowpack or atmosphere. Water input rate varied between 0.25 and 4 mmh^{-1}, thus ranging from low intensity snowmelt to high intensity combined snowmelt and rainfall (Rango and DeWalle, 2008). The total amount of water that was added to the soil was always 80 mm. The thaw/infiltration period therefore lasted from 20 to 320 h depending on the water input rate. Temperature of the water input varied from 0 °C, common for snowmelt, to 2 °C.

In addition to the freeze and thaw scenarios, we performed simulations with the same initial saturation state and the same water input rate but without freezing. These simulations provided the infiltration if there had not been any freezing during the five days prior to water input. The total amount of infiltrated water into the soil column for the freezing scenario was subtracted from the amount of infiltration in the corresponding scenario without freezing; the resulting output variable is called *infiltration change due to freezing*. This variable is of particular interest, as it quantifies the specific effect of freezing on infiltration for a given soil type.

The soil texture classification triangle is shown in Fig. 1 including the position of the soils we simulated. We considered the soil textures simulated to follow a rough gradient from coarse (soil 1) to very fine (soil 8) based on increasing water retention capacity and decreasing permeability. In addition, we considered soils 1 and 2 as coarse soils, soils 3 to 6 as intermediate soils and soils 7 to 8 as very fine soils.

All combinations of conditions in Table 2 were tested for each soil type, except for input water temperature. Water input temperature was initially varied in the simulations (0 to 2 °C), but during testing we found it had no noticeable effect. To limit computational time, we therefore only tested water input temperature for soils 2, 3, 5 and 6.

Thermal conductivity of a soil is dependent on the water content and packing of the grains, their mineral and organic components, their connectivity and their shape (Zhang and Wang, 2017). The relationship with soil texture is therefore complicated. To simplify, we focused on how soil texture affects the infiltration capacity of a frozen soil and assumed all solid grains to have the same thermal conductivity of 2.2 $Wm^{-1}\ K^{-1}$. This represents an arbitrary midpoint value between minerals with a low (e.g. clay minerals and carbonates) and high thermal conductivity (e.g. quartz) (Cermak and Rybach, 1982).

2.3.2. Analysis

A large number of simulation results were obtained from all the scenarios (over 16,000). To visualize the output in a meaningful way, we created boxplots of relevant variables for each soil type. The output variables for the freezing phase were ice saturation of the entire soil profile, average temperature of the topsoil (upper 10 cm) and frost depth (the maximum depth at which ice is present). These boxplots provided insight into the effect of freezing by showing the full range of results as well as the medians and quartiles. Regarding the output of the infiltration phase, boxplots were made for the total amount of infiltration during non-frozen conditions and the total amount of infiltration change due to freezing specifically. In addition, we plot the frequency of cases (%) for each soil type with 0, 25, 50 and 75% infiltration reduction due to freezing (function used: $-100\frac{Infiltration\ change\ (mm)}{Total\ water\ input\ (80\ mm)}$). We also included time plots of cumulative infiltration, ice saturation and total saturation for a few chosen scenarios to illustrate different temporal infiltration regimes.

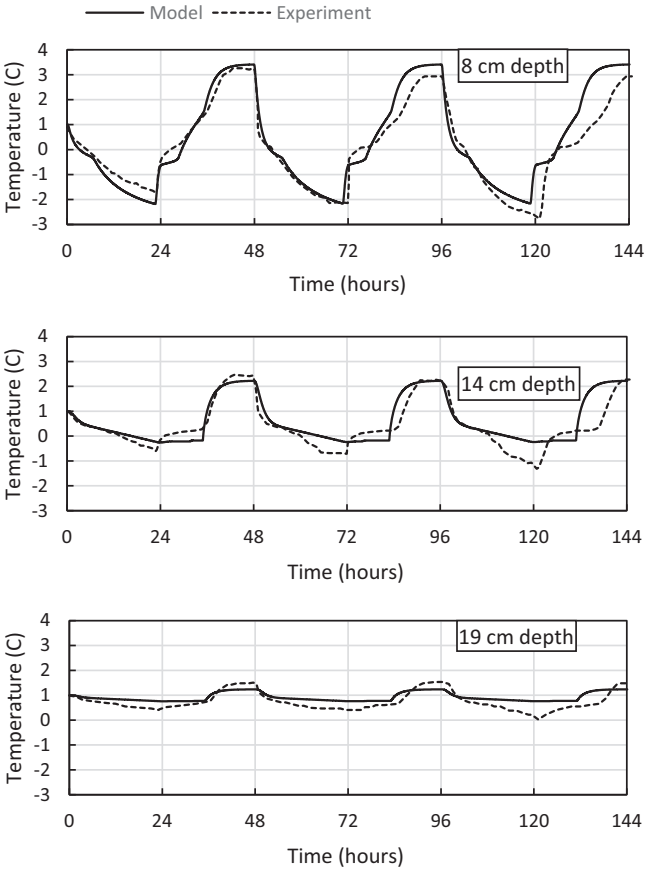

Fig. 2. Measured soil temperatures at 8, 14 and 19 cm depth during repeated freeze-thaw cycles in the experiment by Wang et al. (2017) compared to the simulated temperature of the model.

To get a better overview of the importance of the different environmental parameters for each soil type, we performed Spearman's rho correlation tests between infiltration change and each of the scenario variables (initial saturation, boundary temperature, water input rate and water input temperature). This test was preferred over the linear Pearson's correlation test because we expect a non-linear response in view of the non-linearity of the equations (e.g., soil freezing curve (Eq. (3)), cryosuction (Eq. (2)) and the Richards equation). We plotted the median values of infiltration reduction for each variable value to identify the shape of the relationship between variables and infiltration reduction for each soil type. Finally, we made cross-tabulations for the frequency of cases with over 75% infiltration reduction for each variable combination. These are provided in the Appendix. The cross-tabulations help identify thresholds for extreme infiltration reduction to occur.

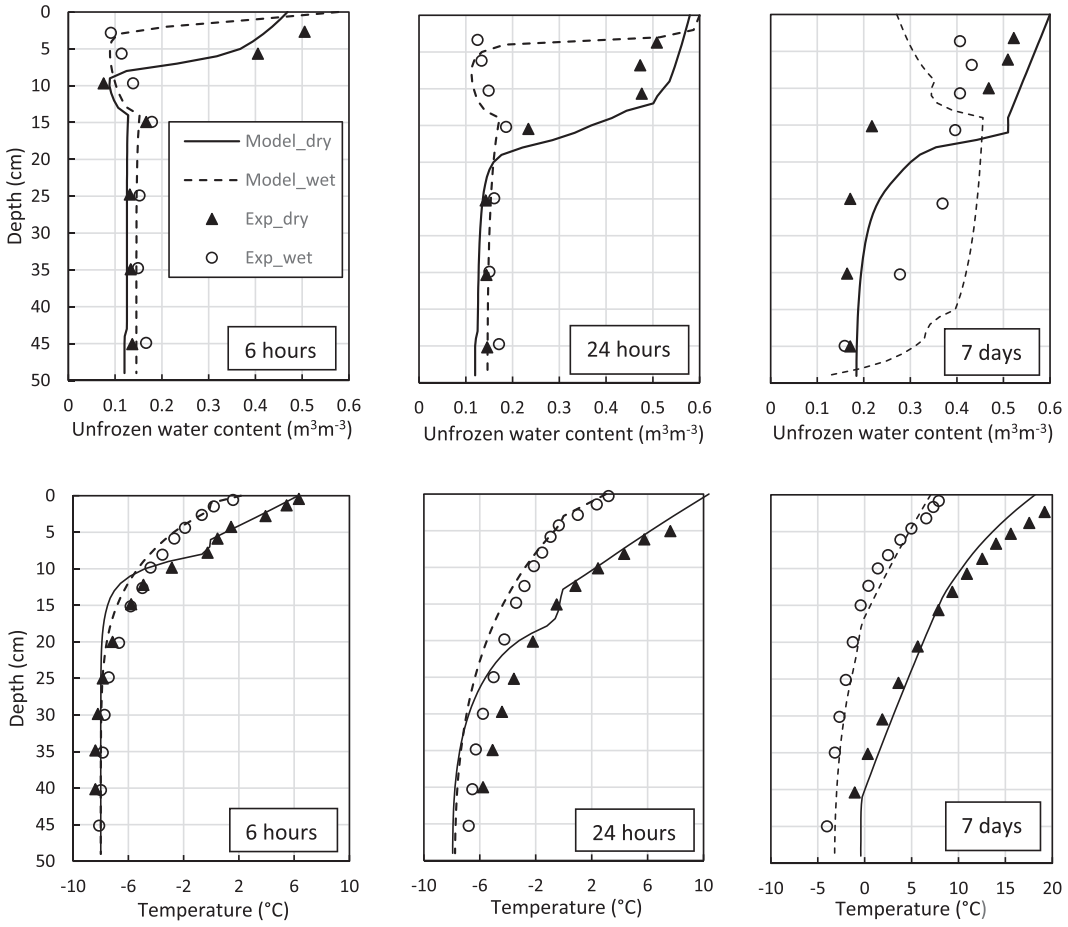

Fig. 3. Comparison of model output with the measurements of Pittman et al. (2020) for both initially dry and wet frozen soil infiltration experiments. Exp stands for experimental measurements.

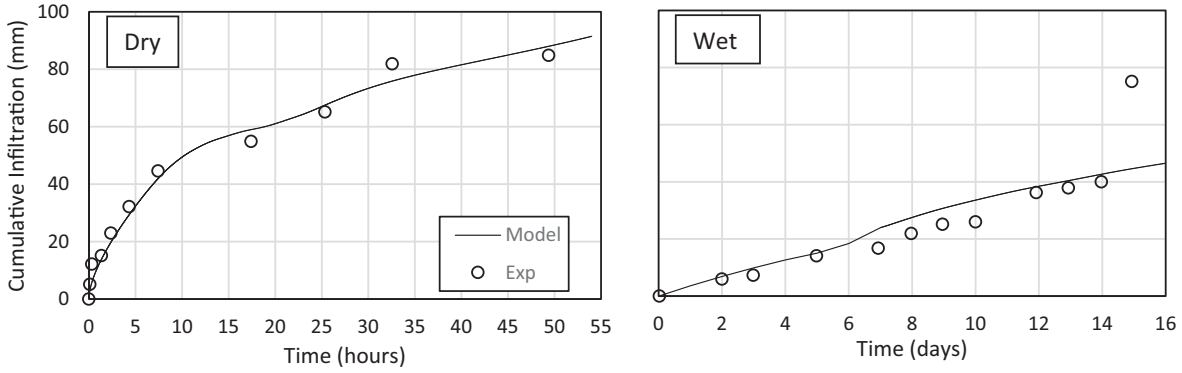

Fig. 4. Plots of measured and modelled cumulative infiltration for initially dry (left) and wet (right) frozen soil experiments of Pittman et al. (2020). Exp stands for experimental measurements.

3. Results & discussion

3.1. Experimental validation

The temperature profiles obtained from the simulations were in good agreement with measured temperatures during the first 48 h at all three depths in the experiment of Wang et al., 2017 (Fig. 2). This provides confidence that the freezing and thawing thermodynamic process was represented well by the numerical model. The increasing deviations after repeated freeze-thaw cycles we attributed to frost heave in the soil column of Wang et al. (2017). Frost heave alters pore and solid particle connectivity and general soil structure, thereby changing the soil's thermal conductivity. It also affects heat capacity and latent heat flux due to the creation of ice lenses. Consequently, the thermal properties of the soil become time-variant (in addition to changes in water, ice and air saturation) and asynchronous temperature cycles can be expected. An alternative explanation for the increased discrepancy could be imperfections in boundary temperature control of the experiment.

The comparison of model output with the experimental data of Pittman et al. (2020) is shown in Figs. 3 and 4. The values of soil

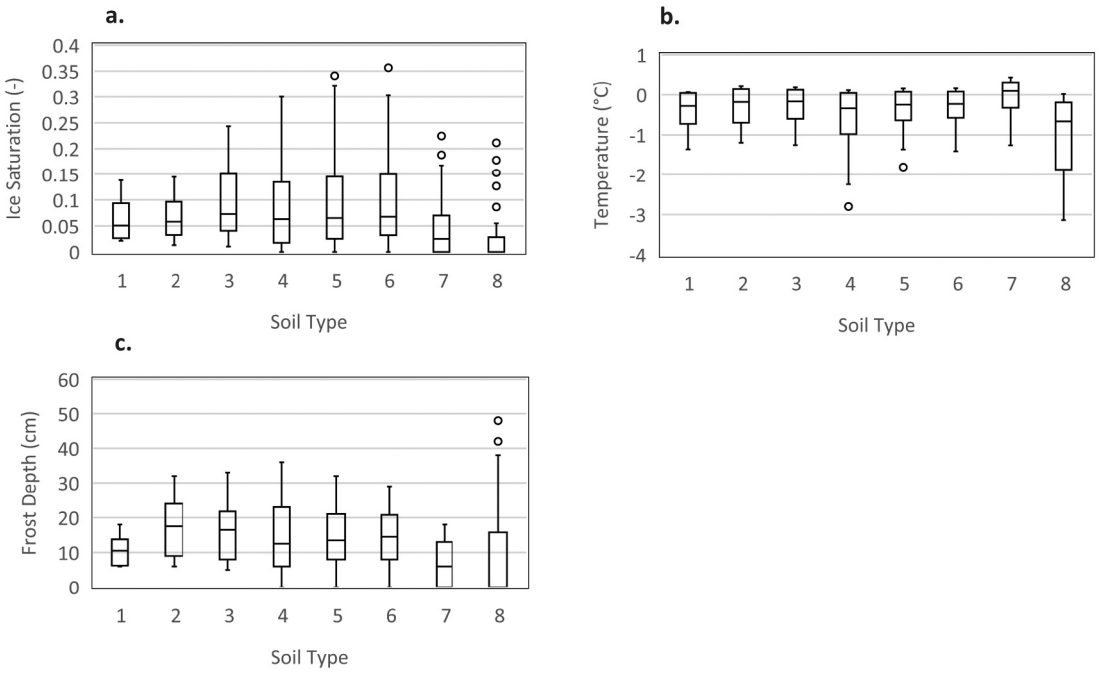

Fig. 5. Boxplots of simulation results at the end of the freezing phase for each soil type of a) ice saturation; b) average temperature of the topsoil (upper 10 cm); c) frost depth.

properties used in these simulations are given in Table 4. Simulated results of unfrozen water content and temperature generally agreed well with the experimental data for both wet and dry initial conditions. Also, cumulative infiltration results of the model corresponded well to the measurements. Despite the calibration involved to represent the experimental setup, these results provided confidence in the ability of the model to simulate the physics of infiltration into frozen soil, regarding both unfrozen water content and temperature development. However, the model failed to predict the unfrozen water content and temperature well after 7 days. This was likely due to an incongruence between soil properties in the experiment and calibrated or estimated soil properties in the simulation which becomes more apparent at longer runtimes. In addition, thermal boundary conditions were not accurately represented by the model because of uncertainty in the amount of radiation that heats up the topsoil, as well as the uncertainty of the amount of energy provided by the bottom heat source.

3.2. Numerical experiments

Here we discuss the results of synthetic testing of different combinations of soil properties and boundary conditions. We describe the results of the freezing phase and the infiltration phase separately.

3.2.1. Differences after the freezing phase

The state of the soil at the end of the freezing phase is summarized in Fig. 5. We separately show the ice saturation (of the entire soil column), frost depth and average temperature in the topsoil (upper 10 cm). A case refers to a specific combination of the variables initial saturation and freezing temperature for a soil type.

3.2.1.1. Ice saturation. It is apparent that soils with intermediate texture (soils 3–6) had the highest ice saturation after the freezing phase when looking at all cases combined in the boxplots; this concerns medians, upper quartiles and outliers (Fig. 5a). These were the only soils which have cases with over 25% of the entire column saturated with ice. In comparison, the coarsest soils, soils 1 and 2, never had more than about 14% ice saturation of the column. With the very fine textured soils, soil 7 and 8, we observed the lowest medians of ice saturation, 0 and 3% respectively. Nevertheless, these soils had outlier cases in which ice saturation exceeded 15%. Furthermore, it was notable that the lowest value of ice saturation is higher for the coarse soils 1 and 2 (ca. 4%), while it was approximately 0% for the other soils. Lastly, we observed that the variability in ice saturation was highest for the intermediate soils.

These results demonstrated that intermediate soil textures potentially have higher ice saturation after the freezing phase compared to coarse and very fine soils. Given the large variability of the output, these soils were most sensitive to initial and boundary conditions. Characteristic of intermediate soils is that they have substantial water retention capacity, which prevents most of the pore water from flowing away due to gravity. Consequently, the pore water can freeze before it is drained. At the same time, the matric pressure is not that strong to reduce the freezing point of water significantly, i.e., the soil freezing curve allows freezing to occur at mild subzero temperature. Lastly, these soils are most susceptible to cryosuction due to moderate permeability combined with substantial water retention. This leads to increases in total water

Table 3
Initial and boundary conditions used in the simulations.

Variable	Value 1	Value 2	Value 3	Value 4	Value 5	Value 6	Value 7	Value 8
Initial total water saturation	0.25	0.3	0.4	0.5	0.6	0.75	0.9	1
Freezing temperature (°C)	−0.25	−0.5	−1	−2	−3	−4		
Thawing temperature (°C)	0	0.5	1	2	3	4		
Water input rate (mmh^{-1})	0.25	0.5	1	2	3	4		
Water input temperature (°C)	0	0.5	1	2				

Table 4
Soil parameters used in the simulation of the frozen soil infiltration experiment by Pittman et al. (2020).

Soil layer (depth)	a (cm^{-1})	n	Ksat (ms^{-1})	Res. Water content	Thermal conductivity solid grain ($Wm^{-1}K^{-1}$)	Porosity
0–15 cm	0.53	1.56	6.27e-07	0.02	1	0.6
15–50 cm	0.04	1.61	1.97e-08	0.08	1	0.51

saturation and hence ice saturation in the freezing topsoil (e.g., Unold and Derk, 2017).

With the coarse soils, gravitational drainage leaves less pore water available for freezing. Small amounts of ice however always form during subzero temperature conditions. The reason is likely that the freezing point of water remains close to 0 °C in these coarse soils due to weak matric pressure, allowing the remaining pore water to freeze. Contrarily, with the very fine soils, the freezing point of water is depressed strongly due to high matric pressure which prevents a substantial amount of water from freezing. Only when the temperature for these soils becomes low enough, i.e., beneath the adjusted freezing point of water, phase change occurs.

3.2.1.2. Topsoil temperature. We focus on the topsoil (upper 10 cm) because this is where most of the thermodynamic freezing process occurs. Differences amongst soil types were observed in the lowering of topsoil temperature during the freezing phase, but there was no clear pattern related to soil texture. Instead, specific soil properties (Table 3) seem to have affected the heat transfer. Topsoil temperature was similar for soils 1 to 6, with soil 4 as a notable exception (Fig. 5b). The sandy clay loam (soil 4) likely stood out as colder than the other soils after the freezing phase due to its low porosity combined with high residual water content. Low porosity implies a higher thermal conductivity because the solid particles have the highest thermal conductivity of all the soil constituents. The heat from the soil is therefore lost relatively rapid when the atmosphere (or snowpack) above is colder. Furthermore, low porosity results in a lower heat capacity due to the limited space for water. A high residual water content means that a significant portion of soil water always remains unfrozen, therefore involving less phase change. The reduction in latent heat flux facilitates temperature change.

For similar reasons prescribed to low porosity, the simulated silty clay (soil 8) became the coldest soil of all soils after the freezing phase. In addition, ice saturation with soil 8 was lowest due to the strong depression of the freezing point of water. This means there hardly was a latent heat flux, allowing for rapid soil cooling. It was also noticeable that the low porosity soils were associated with higher sensitivity to the boundary temperature exemplified by the large variability in topsoil temperature output of soils 4 and 8.

Another anomalous topsoil temperature result could be seen with soil 7, the organic-rich soil. It had the highest median topsoil temperature and it was the only soil with frequent positive topsoil temperature cases at the end of the freezing phase. This is likely also explained by porosity as soil 7 had a high porosity (0.766). The large heat capacity of a water-logged highly porous soil slows down temperature change. At the same time, at low water saturation and thus high air saturation, the thermal conductivity is very low which also slows down freezing. It is not explained by a higher latent heat flux due to more pore water, since ice saturation after freezing was low for this soil.

3.2.1.3. Frost depth. The pattern of frost depth results across soil types was different than the pattern of topsoil temperature results across soil types (Fig. 5c). The frost depth was overall quite similar, but deepest with soils 2 to 6 for most cases (between 0 and 35 cm deep). Soil 7 had the least deep frost, likely because of the high porosity of the soil which leads to relatively warm soil temperature. Soil 8 on the other hand had exceptional outliers with deep frost (up to 49 cm deep). The freezing point of water was low in this soil type (silty clay). As a result, the ice saturation remained low with little latent heat flux, which made it possible to reduce the temperature in the deepest layers.

The minimum value of frost depth seen across cases was a bit deeper with soils 1, 2 and 3 compared to the other soils. Some ice always formed in these soils even with modest freezing temperatures because the freezing point of water was close to the freezing point of water at standard atmospheric pressure. Yet these soils did not have deep frost, likely because rapid drainage prior to freezing left the soil highly saturated with air. The air-filled topsoil acted as an insulator, slowing down the penetration of the freezing front.

3.3. Infiltration results

3.3.1. Overall results for the various soil types

The unfrozen infiltration reference scenarios showed that the total amount of added water, 80 mm, always infiltrated with soils 1 to 4 (Fig. 6a). Soil 5 had only a few unfrozen cases when not all water is infiltrating. With soils 6 and 7, infiltration during nonfrozen conditions varied from half to all the input water. Soil 8 never showed complete infiltration in the unfrozen scenarios with infiltration ranging from nothing to about half of all input water. These results were expected based on the lower permeability of the finer soil textures.

For the partly frozen scenarios, only with soil 1 (sandy soil) the total amount of added water infiltrated in all cases (Fig. 5b). The output for the other soils varied widely: ranging from cases with no infiltration to cases with full infiltration due to freezing. Differences across soil types were large. Firstly, soil 2 and 3 had infiltration reduction occurring only as outlier cases, meaning that specific circumstances were required to see an effect of freezing on infiltration. Secondly, soils in the intermediate texture range (soils 4 to 6) displayed the strongest reduction of infiltration due to freezing. Thirdly, regarding the finer soils, substantial

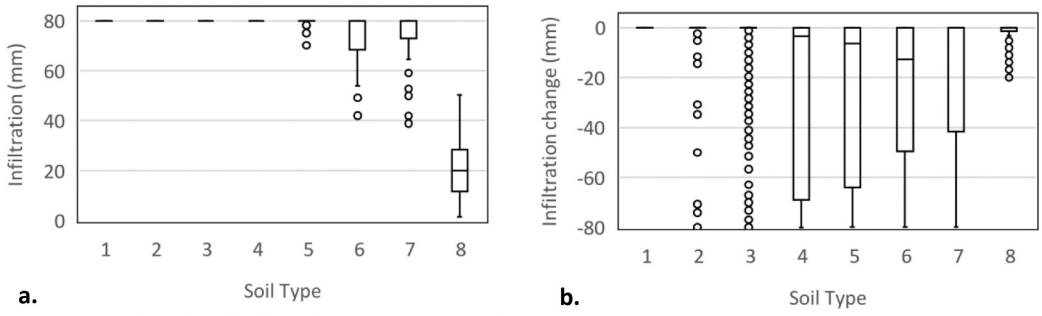

Fig. 6. Boxplots for each soil type of a) amount of infiltration (mm) of input water under non-frozen conditions; b) the change in the amount of infiltration (mm) due to freezing relative to the non-frozen infiltration.

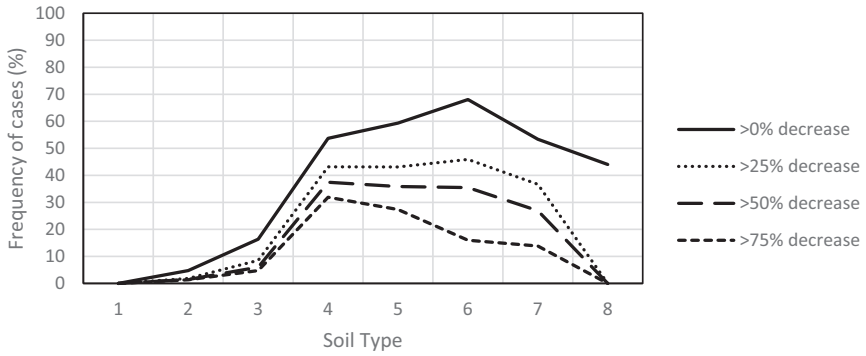

Fig. 7. Graph showing the frequency of simulated cases (%) for each soil type in which a certain amount of infiltration reduction (% of total water input) due to freezing occurred.

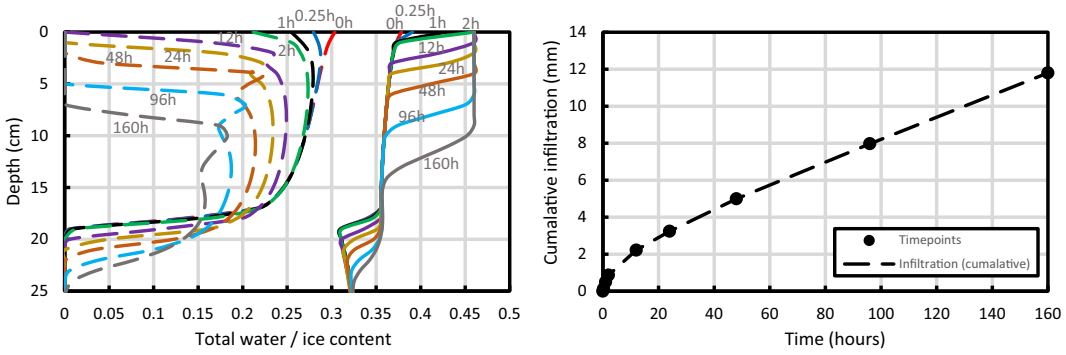

a. Soil 7, initial saturation: 0.75, freezing temperature: -3 °C, thawing temperature: 0.5 °C, inflow rate: 0.5 mmh^{-1}.

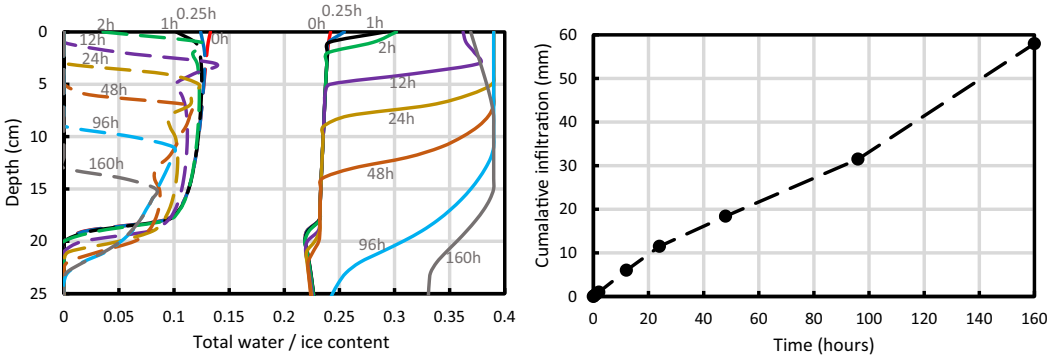

b. Soil 4, initial saturation: 0.6, freezing temperature: -2 °C, thawing temperature: 0.5 °C, inflow rate: 0.5 mmh^{-1}.

Fig. 8. Plots of total water and ice saturation through time, as well as cumulative infiltration, for different scenarios and soil types (a-d). These are selected examples to demonstrate different temporal frozen soil infiltration regimes.

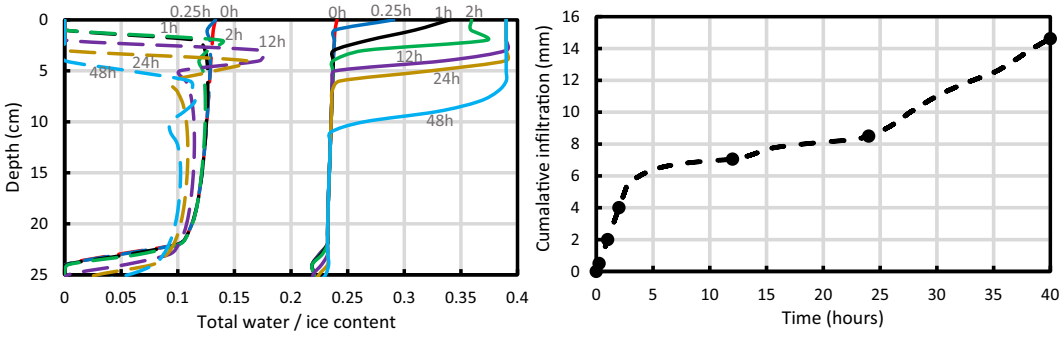

c. Soil 4, initial saturation: 0.6, freezing temperature: -3 °C, thawing temperature: 0.5 °C, inflow rate: 2 mmh^{-1}.

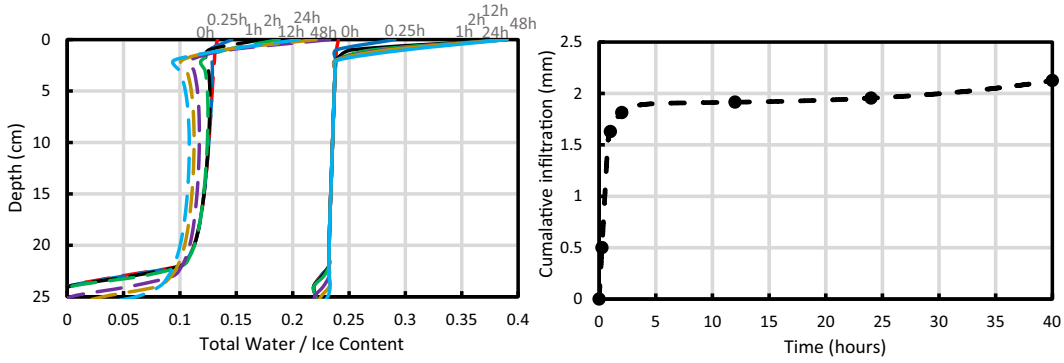

d. Soil 4, initial saturation: 0.6, freezing temperature: -3 °C, thawing temperature: 0 °C, inflow rate: 2 mmh^{-1}.

Fig. 8. (*continued*).

infiltration reduction occured with soil 7 but only to a small extent with soil 8.

The general pattern of strong infiltration reduction due to freezing for the intermediate soils was confirmed in Fig. 7, in which the frequency of cases with a certain severity of infiltration reduction due to freezing is shown. Soil 4 had the highest frequency of cases (ca. 30%) in which infiltration reduction due to freezing was over 75% of the input water. Concludingly, the sandy clay loam (soil 4) was most severely affected in its infiltration capacity by freezing in our study.

The main reason for the major effect of freezing on infiltration capacity of intermediate soils (soils 4 to 6 specifically) is the substantial ice saturation of these soils caused by freezing as observed in the previous section. The high ice saturation results in a strong drop in permeability and reduced accommodation space for infiltrating water. Importantly, these soils are during unfrozen conditions already near the threshold for infiltration excess overflow for various input rates, hence the permeability drop due to ice has significant impact. These results add information to the general notion that loamy and silty soils are most susceptible to the process of cryosuction and frost heaving (Hansson and Lundin, 2006).

Coarse soils have low ice saturation and hence higher permeability and more space for infiltrating water, leading to the result that freezing had little to no effect on infiltration. The infiltration into the silty clay (soil 8) was only mildly affected by freezing because of two major reasons: 1) unfrozen soil infiltration is already inhibited, hence further reduction in permeability has less compounding effect; 2) the freezing point of water is depressed strongly (Eq. (2)), leading to low ice saturation. The same applies to soil 7, the organic rich soil type, but with the exception that in several cases freezing did have a significant effect on infiltration. From the cross-tabulations in the Appendix, it follows that these cases concerned high initial saturation of soil 7 before the freezing phase.

3.3.2. *Temporal infiltration regimes*

Examples of the cumulative infiltration along with the development of ice content and total saturation with time are shown in Fig. 8. These examples are selected to display the two different types of infiltration regime we observed. The example of soil 7 showed a two-phase infiltration pattern: infiltration rate decreased until it reaches a steady rate, similar to frozen soil infiltration as observed by Zhao and Gray (1998). The time it took to reach steady-state infiltration and the steady-state infiltration rate itself varied across cases, but only one example is shown here as this type of infiltration is not different from a normal infiltration curve into an unfrozen soil. First, the infiltration rate

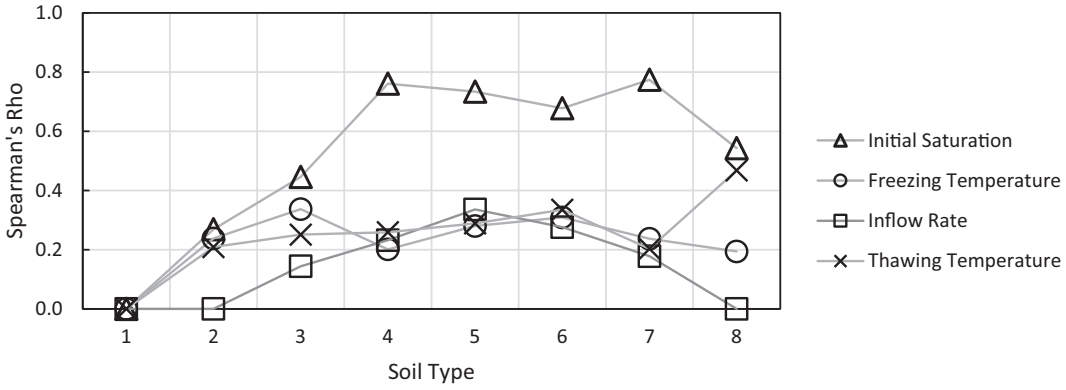

Fig. 9. Plot of the Spearmean's Rho correlation coefficients for the relationship between each environmental variable and the reduction in infiltration due to freezing for each soil type ($p < 0.01$). Non-significant correlation coefficients ($p > 0.01$) were plotted as 0.

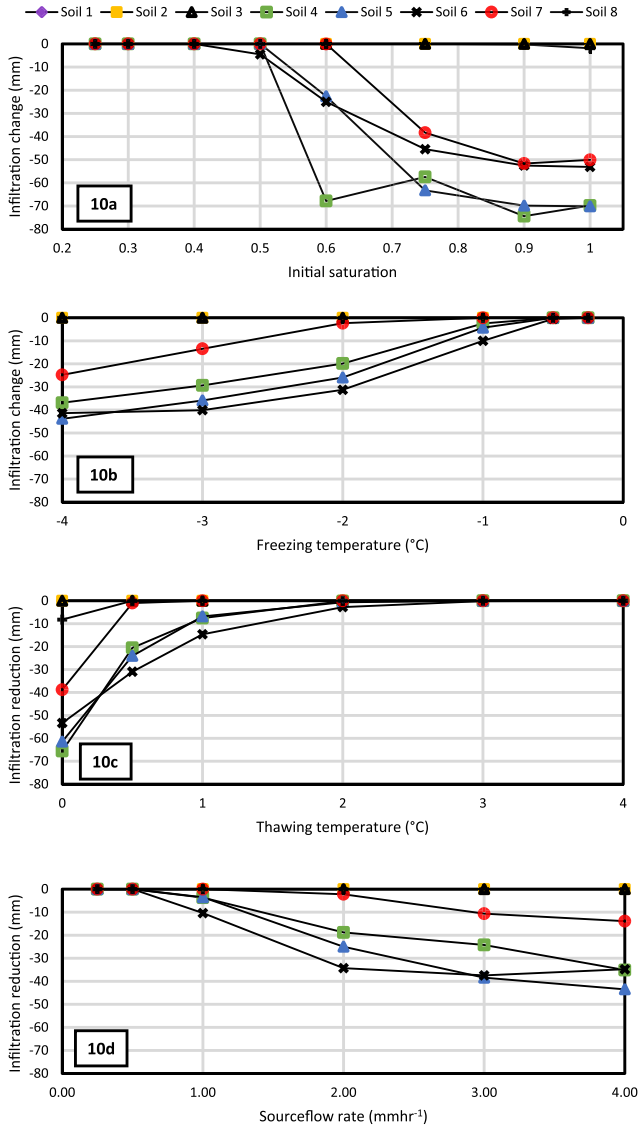

Fig. 10. Median values of infiltration reduction due to freezing (%) for input variable values of initial saturation (a), freezing temperature (b), thawing temperature (c) and inflow rate (d).

gradually decreased as the matric pressure gradient becomes smaller. The second phase was characterized by a steady-state infiltration through the frozen zone at a rate lower than the saturated hydraulic conductivity due to the presence of ice. The heat transfer due to soil warming aligned with the progression of the wetting front as the ice rich zone lies exactly beneath the wetting front for all timepoints. The thawing rate was thus dictated by the maximum infiltration rate.

It could be expected that during prolonged infiltration, the wetting front eventually would reach the unfrozen zone. At this point, infiltration would likely accelerate, but this was not observed within the simulated time periods of this study (maximum 320 h). Below the wetting front, we observed that the ice melted at a consistent pace, likely due to heat from deeper and warmer layers in the soil. The meltwater then refroze deeper where the soil is still in the process of cooling. This phenomenon of downward ice migration occured in both infiltration regimes, and it can be expected as soon as freezing from the top stops.

A three-phase infiltration regime could be observed in the examples of soil 4: first infiltration slowed down, followed by a temporary steady infiltration rate, and finally an increased infiltration rate until a steady-state situation. However, the results for the three different cases of soil 4 shown in Fig. 8 varied a lot both in length of the different phases and in their infiltration rates. In the case of Fig. 8b, there was a modest increase in ice saturation after 1 h causing the penetration of the wetting front to slow down in phase 2. It turned into a slightly higher steady-state infiltration rate again when thawing causes most of this increased ice saturation below the wetting front to disappear after 96 h.

A large local increase in ice saturation could be observed in Fig. 8c, when the soil had been frozen more severely (−3 instead of −2 °C) and the input rate was higher (2 instead of 0.5 mmh^{-1}). The colder soil and faster addition of water caused significant freezing of infiltrating water. Consequently, the wetting front hardly moved downward during phase 2. During this phase, most of the infiltration excess overland flow could be expected. The final phase starts when the heat from above connected to the ice rich layer and caused it to thaw. As a result, the infiltration rate increased. The slightly wobbly pattern observed in the plot was likely an artefact of numerical discretization of the thin highly ice-saturated layer.

In the case of Fig. 8d, the increase in ice saturation was severe and occurred immediately in the top few centimeters of the soil. This was the result of near absence of thaw (0 °C top temperature boundary) resulting in a quick halt of the wetting front at the frozen infiltrated water layer. After 24 h the heat from the top boundary temperature slowly initiated melting. The infiltration rate thereby transitioned to phase 3 but not clearly within the timespan of the simulated water input event. Only about 2 of the 80 mm water infiltrated, meaning that most of the melt- and rainwater became surface runoff.

The three-phase infiltration regime is different from the three frozen soil infiltration phases described by Watanabe et al. (2013). They

observed the first phase as having no infiltration at all, followed by slow infiltration and rapid infiltration, respectively. It is possible the different first phase of the infiltration regime in their experiment was the consequence of a permanent 15-cm constant head at the top of the column, causing instant sealing of the topsoil due to in-situ freezing. A more realistic slow water input rate does not lead to such immediate ice sealing, instead the local ice saturation increases gradually, allowing infiltration during the first phase. Additionally, the topsoil boundary had a temperature of −6 °C in the experiment of Watanabe et al. (2013), leading to rapid in-situ freezing. This might be unrealistically cold for most field situations.

3.4. Scenario variables

The scenario variables studied include initial saturation, freezing temperature, thawing temperature, water input rate and water input temperature. The statistically significant Spearman correlation coefficients for the relationship between the variables and infiltration change for each soil type are plotted in Fig. 9 ($p < 0.01$). All correlations that were not significant ($p \geq 0.01$) were put to a value of 0 (i.e., no relationship). Input water temperature had no significant Spearman correlation with infiltration change due to freezing for all soils ($p > 0.01$). It is therefore omitted from Figs. 9 and 10. The median values of infiltration change due to freezing are plotted in Fig. 10 against each of the other variable values. In the appendix, the frequency of cases with extreme infiltration reduction due to freezing (>75%) are shown for each combination of variable values.

3.4.1. Initial saturation

In our simulations, initial saturation was the most important factor determining the impact of freezing on infiltration into frozen ground (Fig. 9), a similar finding as other studies (e.g., Watanabe and Osada, 2017; Zhao et al., 2013). A particularly strong relationship between reduced infiltration and initial saturation existed for soils 4 to 7 (Spearman's rho >0.6). The more pore water initially present, the higher the potential ice saturation and the more the permeability and accommodation space for infiltrating water are reduced.

With soil 4 however, median infiltration reduction was weaker at 0.75 than at 0.6 initial saturation, and weaker at 1.0 than at 0.9 initial saturation, resulting in a sinusoidal type of relationship between 0.6 and 1.0 initial saturation (Fig. 10a). The same pattern could be found in the cross-tabulations in the Appendix, in which different variable combinations are shown. This effect of higher initial saturation seemed to occur irrespective of the values of the other variables. With soil 7 a similar phenomenon could be observed as the median infiltration reduction is weaker at 1.0 than at 0.9 initial saturation (Fig. 10a). This phenomenon could be explained by the presence of two opposing processes: an increase in latent heat flux and heat capacity due to more initial pore water slows down temperature change leading to lower ice saturation, while more initial porewater also causes higher thermal conductivity and potentially higher ice saturation since more loosely held water is available. Apparently at these specific higher initial saturation values, the energy cost is stronger than the potential volumetric increase in ice saturation. This finding demonstrates the sensitivity of the freezing process to specific circumstances, antecedent conditions, and the intricate balance of processes involved.

3.4.2. Freezing temperature

A temperature threshold could be identified for most soils; above this value, infiltration change due to freezing was minimal. Below the threshold, the relationship between freezing temperature and median infiltration change was mostly linear with gradually more infiltration reduction with decreasing temperature (Fig. 10b). The threshold was at −0.5 °C for soils 4, 5 and 6, while with soil 7 it lies at −2 °C. For the other soils, no relationship could be observed due to the low number of cases with infiltration change. The decrease in infiltration with lower temperature below the threshold could be explained by a few factors. The lower the temperature of the soil, the higher the potential ice saturation as dictated by the soil freezing curve. Also, the faster freezing rate at lower temperature means that water can be immobilized quicker before it drains. Furthermore, a colder soil thaws slower and has more potential to experience infiltrating water freezing in-situ.

3.4.3. Thawing temperature

A non-linear relationship could be observed between thawing temperature and median infiltration change for most soils (Fig. 10c). Increasing the thawing temperature from 0 to 1 °C substantially decreased the number of cases with strong infiltration reduction due to freezing. Above 1 °C (0.5 °C for soils 7 and 8), an even higher thawing temperature had less effect. The crucial temperature range for effective thaw thus seemed to lie between 0.5 and 1 °C for most soils. Above the threshold boundary temperature sufficient energy was transferred to raise the soil temperature above the freezing point of water. If the boundary temperature was too low, the soil remains cold and frozen, and the potential for infiltrating water freezing in-situ is high. In practice, infiltration is therefore strongly inhibited when a snowpack exists on top of the soil. A melting snowpack has a temperature of about 0 °C (Rango and DeWalle, 2008), while the soil itself is insulated from the air. Top boundary thawing temperatures above 0 °C represent situations with snowpack free conditions whereby the atmosphere and solar radiation provide energy to the soil. In those cases, frozen soil infiltration can be much enhanced due to thaw.

3.4.4. Inflow rate

Intermediate soil textures displayed a stronger correlation between inflow rate and infiltration change due to freezing than both finer and coarser soils. The correlation only existed for soils 3 to 7, ranging from a Spearman's rho of 0.17 for soil 3 to about 0.32 for soil 5 (Fig. 9). A threshold for the effect on median infiltration change could also be observed (Fig. 10d). The strongest decrease in infiltration occurred between 0.5 and 2 mmh^{-1} water input with soils 4 to 6. Below 0.5 mmh^{-1} input rate, the median infiltration change was zero. Above 2 mmh^{-1}, the effect of higher input rate diminished, except for soil 7. The role of water input rate thus seemed straightforward: the higher the input rate, the more likely it was that the infiltration capacity of frozen soil is exceeded. However, with soils that already experience infiltration rate excess during the unfrozen reference scenarios, a very high input rate leads to a comparatively less strong effect of pore ice on infiltration.

Concludingly, with a low water input rate, water can often still infiltrate into frozen soil. However, the data in the Appendix showed that infiltration could still be severely inhibited if the soil is highly saturated before freezing, or if the soil is cold enough to cause freezing of infiltrating water.

3.4.5. Extreme cases

The appendix displays the cross-tabulations for each variable combination and the frequency of cases with over 75% infiltration reduction due to freezing. The highest number of cases was for most soils associated with a low boundary thawing temperature, especially at 0 °C. This underscores the importance of thawing and the opposing process of infiltrating water freezing in-situ with its effect on subsequent infiltration. Infiltrating water freezes readily in still frozen soil because the available pore space has less matric pressure. Furthermore, most of the extreme cases occurred when freezing temperature was lower than −0.5

or − 1 °C and initial saturation was at least 0.6 or 0.75. In some cases, such as with soil 4, a higher initial saturation (0.75 compared to 0.6, and 1.0 compared to 0.9) corresponded to less extreme infiltration reduction cases. This is similar to the earlier finding on the effect of specific values of higher initial saturation. In practice, the extreme cases show the conditions during which flood and erosion risk are highest.

3.5. Uncertainty

This study did not include simulation of preferential flow through macropores. It has been found in previous studies that macropores often allow infiltration to occur uninhibited into a frozen soil because macropores rarely saturate with ice (Mohammed et al., 2018). Under specific circumstances, infiltrating water could however freeze within macropores and lead to ice blockage of preferential flow (Mohammed et al., 2021). Despite the importance of macropores for frozen soil infiltration, the focus of this study is on the soil matrix and the effect of various single-domain soil parameters.

Also not considered in this study was alteration of pore structure due to frost heave. The prediction of frost heave has received a lot of attention (Lein et al., 2019), but there is less knowledge of its influence on soil hydrological properties. An experimental study by Leuther and Schlüter (2021) shows that clay content is important in determining the effect of freeze-thaw cycles on pore structure. They also demonstrate changes in soil water retention and hydraulic conductivity due to soil structure change. There is however too little empirical information yet to derive constitutive relationships between soil freezing and soil hydrological properties.

Furthermore, it is uncertain whether the empirical parameter Ck for cryosuction (Eq. (1)) had a value of 1.8 for all soil types due to lack of empirical data. Based on Stuurop et al. (2021) it is however suggested that Ck functions as a constant independent of soil texture. Lastly, soil thermal conductivity between soil types in our simulations could only differ due to differences in porosity and water, ice, and air content. Although these are major factors determining soil thermal conductivity, other possible changes in thermal conductivity were not considered such as different solid grain thermal conductivities.

3.6. Outlook

The modelling exercise performed in this study provided several clues as to how temperature, soil texture, initial water content and water input rate play a role in determining frozen soil infiltration capacity. These are theoretical results based on the equations that represent the thermodynamics of freezing and thawing as well as transport of water in porous media. Further empirical validation is needed based on experimental work. This study could provide a framework for more focused experiments to expand the empirical knowledge on frozen soil infiltration. Similar soil types could for example be used to verify that infiltration into intermediate textured soils is most affected. The same boundary and initial conditions could be recreated for a smaller number of test columns, to investigate if similar effects as we have modelled are observed. Of particular interest could be the role initial saturation plays, as well as the importance of freezing of infiltrating water.

4. Conclusion

Comparison with experimental data suggested the model is capable of simulating infiltration into frozen soil. Numerical simulation of a high number of synthetic test cases provided insight into the freezing, thawing and infiltration process of various soil types during different boundary conditions. The most important findings are listed below.

- Intermediate soil textures had the highest ice saturation after the freezing phase compared to coarse and fine soils and therefore the strongest reduction in infiltration capacity due to freezing. Coarse soils were hardly affected but very fine soils to some extent depending on specific conditions.
- A two-phase infiltration regime existed when the thawing front during infiltration did not overtake the wetting front and no significant amount of infiltrating water froze in-situ. At first, infiltration was fast until the soil was highly saturated. Subsequently, there was slow steady-state infiltration through the frozen zone. This infiltration pattern is similar to normal infiltration into unfrozen soil.
- A three-phase infiltration regime existed when a substantial amount of infiltrating water froze in-situ. First, infiltration rate decreased as ice saturation increased. Secondly, there was quasi-steady state infiltration with a very slow rate due to frozen infiltrated water. Thirdly, infiltration rate increased when the thawing front connected to the frozen infiltrated water. Significant surface runoff could be expected during phase 1 and 2 due to the frozen infiltrated water.
- Large differences existed concerning the effect of environmental parameters (initial saturation, freezing temperature, thawing temperature and water input rate) on frozen soil infiltration for various soil types. Overall, initial saturation was one of the most important factors affecting frozen soil infiltration capacity. Water input temperature had no effect. Threshold values were identified at which frozen soil infiltration capacity started to become increasingly affected, e.g. initial saturation of 0.6 and 0 °C top boundary temperature during infiltration for most intermediate soil types.
- Cases of severe infiltration reduction due to freezing were for most soils associated with an initial saturation of at least 0.6 or 0.75, an absence of thaw (0 °C top boundary temperature) and a freezing temperature of at least −0.5 or − 1 °C for five days; differences between soil types should be considered.
- Low soil porosity facilitated soil cooling and thereby led to increased chances of infiltrating water freezing in-situ, while high porosity slowed down soil cooling.
- Ice migrated slowly downward during the infiltration and thawing phase through refreezing of melted ice deeper in the soil.

The results of this study are based on numerical simulation and therefore provide theoretical insight into the freezing and infiltration dynamics of a homogenous 1-dimensional soil column. The simulations provide a framework for further experimental work to validate or falsify our findings. This study also provides insight into the intricate and complicated physics of frozen soil infiltration with many tipping points and processes steering in different directions. A drawback of our approach is the lack of structural soil change during freezing and the absence of preferential flow. The current reality is that little information exists to be able to predict a change in hydraulic properties due to freeze-thaw cycles. Our results should therefore be considered uncertain for cases in which frost heave is expected. It should also be considered that our results show the link between various parameters in the absence of macropores; the case of preferential flow requires further specific attention.

Declaration of Competing Interest

None.

Appendix A

Cross-tabulations showing the number of cases for each variable combination in which infiltration reduction due to freezing was at least 75%. A red-white colour gradient is applied to each cross-tabulation, with white being the lowest value, red the highest value. The total number of cases in which each variable combination occurred is also given.

Total cases: 36		**Initial Saturation**					
Soil Type	**Freezing Temperature**	0.40	0.50	0.60	0.75	0.90	1.00
2	-4.00				4	4	4
	-3.00				3	4	4
3	-4.00			3	8	9	9
	-3.00			3	5	5	8
	-2.00			2	5	6	6
	-1.00				3	4	3
	-.50					1	2
4	-4.00		5	27	24	34	31
	-3.00		5	27	23	34	30
	-2.00			27	23	31	26
	-1.00			27	16	27	20
	-.50			23	10	22	11
	-.25			20	6	15	7
5	-4.00	2	8	13	27	32	34
	-3.00		5	12	27	31	32
	-2.00		4	11	25	28	29
	-1.00		3	10	19	23	24
	-.50			6	10	15	16
	-.25			3	6	9	9
6	-4.00	3	5	8	16	21	22
	-3.00	2	5	8	15	20	20
	-2.00	1	4	6	13	17	18
	-1.00		2	5	9	11	13
	-.50		1	2	4	7	7
	-.25			1	2	4	4
7	-4.00		2	5	12	22	23
	-3.00		1	5	10	22	22
	-2.00			2	9	19	19
	-1.00			1	6	14	14
	-.50				3	9	9
	-.25				2	4	4
Total cases: 36		**Initial Saturation**					
Soil Type	**Thawing Temperature**	0.40	0.50	0.60	0.75	0.90	1.00
2	.0				7	8	8
3	.0			7	17	21	22
	.5			1	3	3	5
	1.0					1	1
	2.0				1		
4	.0		9	36	33	36	35
	.5		1	34	23	33	26
	1.0			28	17	30	22
	2.0			22	12	26	17
	3.0			17	10	19	13
	4.0			14	7	19	12
5	.0	2	16	27	33	35	35
	.5		4	15	24	30	30
	1.0			11	19	25	25
	2.0			2	15	19	20
	3.0				13	16	18
	4.0				10	13	16
6	.0	6	15	21	21	23	23
	.5		2	6	13	18	18
	1.0			3	10	14	14
	2.0				7	9	12
	3.0				5	9	9
	4.0				3	7	8
7	.0		3	11	20	23	23
	.5			2	10	18	18
	1.0				7	17	17
	2.0				4	14	14
	3.0				1	9	10
	4.0					9	9

Total cases: 36	**Initial Saturation**						
Soil Type	**Inflow rate**	0.4	0.5	0.6	0.75	0.9	1
2	1.00				2	2	2
	2.00				2	2	2
	3.00				2	2	2
	4.00				1	2	2
3	.25					1	2
	.50				3	3	3
	1.00			2	4	4	4
	2.00			3	5	6	7
	3.00			1	5	6	6
	4.00			2	4	5	6
4	.25			1	4	15	8
	.50		2	16	10	22	14
	1.00		2	22	12	27	21
	2.00		2	33	22	31	25
	3.00		3	35	26	34	28
	4.00		1	35	28	34	29
5	.25				4	10	11
	.50		1	4	10	16	18
	1.00		3	6	18	23	24
	2.00	1	5	13	25	28	29
	3.00	1	6	17	28	30	30
	4.00		5	15	29	31	32
6	.25			2	5	10	11
	.50		3	4	10	18	19
	1.00	2	4	7	19	24	25
	2.00	3	7	13	25	28	29
	3.00	1	3	4			
7	.25				3	13	14
	.50			2	7	21	21
	1.00		1	3	14	26	26
	2.00		2	6	18	30	30
	3.00			2			

Total cases: 48	**Thawing temperature**						
Soil Type	**Freezing temperature**	0	0.5	1	2	3	4
2	-4.00	12					
	-3.00	11					
3	-4.00	19	7	2	1		
	-3.00	19	2				
	-2.00	16	3				
	-1.00	10					
	-.50	3					
4	-4.00	28	24	21	18	15	15
	-3.00	28	23	20	19	15	14
	-2.00	24	22	20	16	13	12
	-1.00	24	20	17	13	9	7
	-.50	23	16	12	6	5	4
	-.25	22	12	7	5	2	
5	-4.00	30	24	20	16	14	12
	-3.00	27	21	20	15	13	11
	-2.00	27	20	17	12	11	10
	-1.00	26	17	13	9	8	6
	-.50	21	13	8	4	1	
	-.25	17	8	2			
6	-4.00	24	15	12	9	8	7
	-3.00	23	14	12	8	8	5
	-2.00	21	12	9	7	5	5
	-1.00	18	9	6	4	2	1
	-.50	14	5	2			
	-.25	9	2				
7	-4.00	18	12	10	10	8	6
	-3.00	17	12	10	9	6	6
	-2.00	14	10	10	7	4	4
	-1.00	12	8	7	4	2	2
	-.50	11	4	4	2		
	-.25	8	2				

Total cases: 48		**Inflow rate**					
Soil Type	**Freezing temperature**	0.25	0.5	1	2	3	4
2	-4.00			3	3	3	3
	-3.00			3	3	3	2
3	-4.00	2	3	4	7	6	7
	-3.00	1	3	4	5	5	3
	-2.00		3	3	4	4	5
	-1.00			3	3	3	1
	-.50				2		1
4	-4.00	10	16	20	25	26	24
	-3.00	9	17	19	24	25	25
	-2.00	7	12	17	23	24	24
	-1.00	6	8	13	19	21	23
	-.50	3	6	8	13	18	18
	-.25	2	5	7	9	12	13
5	-4.00	8	16	20	24	25	23
	-3.00	7	13	19	22	24	22
	-2.00	5	9	17	22	22	22
	-1.00	3	6	9	18	21	22
	-.50	2	3	6	9	13	14
	-.25		2	3	6	7	9
6	-4.00	10	17	21	24	3	
	-3.00	8	15	21	24	2	
	-2.00	5	11	18	23	2	
	-1.00	3	6	12	18	1	
	-.50	2	3	6	10		
	-.25		2	3	6		
7	-4.00	10	15	18	20	1	
	-3.00	9	15	16	19	1	
	-2.00	7	9	16	17		
	-1.00	2	7	10	16		
	-.50	2	3	7	9		
	-.25		2	3	5		

Total cases: 48		**Inflow rate**					
Soil Type	**Thawing temperature**	0.25	0.5	1	2	3	4
2	.0			6	6	6	5
3	.0	3	9	14	17	13	11
	.5				4	4	4
	1.0					1	1
	2.0						1
4	.0	21	26	25	26	26	25
	.5	10	17	20	22	24	24
	1.0	4	11	18	20	22	22
	2.0	2	6	11	18	20	20
	3.0		2	5	15	18	19
	4.0		2	5	12	16	17
5	.0	14	22	26	29	29	28
	.5	6	11	15	22	25	24
	1.0	4	8	11	17	19	21
	2.0	1	4	9	12	16	14
	3.0	0	3	8	11	12	13
	4.0	0	1	5	10	11	12
6	.0	16	24	29	32	8	
	.5	7	11	16	23		
	1.0	4	8	12	17		
	2.0	1	5	10	12		
	3.0		4	8	11		
	4.0		2	6	10		
7	.0	13	19	22	24	2	
	.5	6	10	14	18		
	1.0	6	8	13	14		
	2.0	4	6	9	13		
	3.0	1	4	6	9		
	4.0		4	6	8		

References

Ala-Aho, P., Autio, A., Bhattacharjee, J., Isokangas, E., Kujala, K., Marttila, H., Menberu, M., Meriö, L.-J., Postila, H., Rauhala, A., Ronkanen, A.-K., Rossi, P.M., Saari, M., Torabi Haghighi, A., Kløve, B., 2021. What conditions favor the influence of seasonally frozen ground on hydrological partitioning? A systematic review. Environ. Res. Lett. 16, 043008 https://doi.org/10.1088/1748-9326/abe82c.

Azmatch, T.F., Sego, D.C., Arenson, L.U., Biggar, K.W., 2012. New ice lens initiation condition for frost heave in fine-grained soils. Cold Reg. Sci. Technol. 82, 8–13. https://doi.org/10.1016/j.coldregions.2012.05.003.

Blackburn, W.H., Pierson, F.B., Seyfried, M.S., 1990. Spatial and temporal influence of soil frost on infiltration and erosion of sagebrush rangelands. J. Am. Water Resour. Assoc. 26, 991–997. https://doi.org/10.1111/j.1752-1688.1990.tb01434.x.

Carsel, R.F., Parrish, R.S., 1988. Developing joint probability-distributions of soil-water retention characteristics. Water Resour. Res. 24 (5), 755–769. https://doi.org/10.1029/WR024i005p00755.

Cermak, V., Rybach, L., 1982. Thermal properties. In: Angenheister, G., Cermák, V., Hellwege, K.-H., Landolt, H. (Eds.), Zahlenwerte und Funktionen aus Naturwissenschaft und Technik: Neue Serie. — Numerical Data and Functional Relationships in Science and Technology: New Series c. Springer, Berlin, pp. 310–314.

Coles, A.E., McDonnell, J.J., 2018. Fill and spill drives runoff connectivity over frozen ground. J. Hydrol. 558, 115–128. https://doi.org/10.1016/j.jhydrol.2018.01.016.

French, H.K., Binley, A., 2004. Snowmelt infiltration: monitoring temporal and spatial variability using time-lapse electrical resistivity. Journal of Hydrology 297 (1), 174–186. https://doi.org/10.1016/j.jhydrol.2004.04.005. In press.

French, H.K., Hardbattle, C., Binley, A., Winship, P., Jakobsen, L., 2002. Monitoring snowmelt induced unsaturated flow and transport using electrical resistivity tomography. J. Hydrol. 267 (3-4), 273–284. https://doi.org/10.1016/S0022-1694(02)00156-7.

Granger, R.J., Gray, D.M., Dyck, G.E., 1984. Snowmelt infiltration to frozen prairie soils. Can. J. Earth Sci. 22, 464–472. https://doi.org/10.1139/e84-073.

Gray, D.M., Granger, R.J., 1986. In situ measurements of moisture and salt movement in freezing soils. Can. J. Earth Sci. 23 (5), 696–704. https://doi.org/10.1139/e86-069.

Hansson, K., Lundin, L., 2006. Equifinality and sensitivity in freezing and thawing simulations of laboratory and in situ data. Cold Reg. Sci. Technol. 44 (1), 20–37.

Hayashi, M., 2013. The cold vadose zone. Hydrological and ecological significance of frozen-soil processes. Vadose Zone J. 12 (4) https://doi.org/10.2136/vzj2013.03.0064.

Ireson, A.M., van der Kamp, G., Ferguson, G., Nachshon, U., Wheater, H.S., 2013. Hydrogeological processes in seasonally frozen northern latitudes: understanding, gaps and challenges. Hydrogeol. J. 21 (1), 53–66. https://doi.org/10.1007/s10040-012-0916-5.

Jones, H.G., Pomeroy, J.W., 2001. Early spring snowmelt in a small boreal forest watershed: influence of concrete frost on the hydrology and chemical composition of streamwaters during rain-on-snow events. In: 58th Eastern Snow Conference Ottawa, Ontario, Canada, pp. 209–218.

Kulik, V.Y., 1978. Water Infiltration into Soil (in Russian). Gidrometeoizdat.

Kurylyk, B.L., Watanabe, K., 2013. The mathematical representation of freezing and thawing processes in variably-saturated, non-deformable soils. Adv. Water Resour. 60, 160–177. https://doi.org/10.1016/j.advwatres.2013.07.016.

Larsbo, M., Holten, R., Stenrød, M., Eklo, O.M., Jarvis, N., 2019. A dual-permeability approach for modeling soil water flow and heat transport during freezing and thawing. Vadose Zone J. 18 https://doi.org/10.2136/vzj2019.01.0012.

Lein, W.A., Slone, S.M., Smith, C.E., Bernier, A.P., 2019. Frost depth penetration and frost heave in frost susceptible soils. In: International Airfield and Highway Pavements Conference 2019.

Leuther, F., Schlüter, S., 2021. Impact of freeze–thaw cycles on soil structure and soil hydraulic properties. SOIL 7, 179–191. https://doi.org/10.5194/soil-7-179-2021.

McCauley, C.A., White, D.M., Lilly, M.R., Nyman, D.M., 2002. A comparison of hydraulic conductivities, permeabilities and infiltration rates in frozen and unfrozen soils. Cold Reg. Sci. Technol. 34 (2), 117–125.

Mohammed, A.A., Kurylyk, B.L., Cey, E.E., Hayashi, M., 2018. Snowmelt infiltration and macropore flow in frozen soils: overview, knowledge gaps, and a conceptual framework. Vadose Zone J. 17 (1), 1–15. https://doi.org/10.2136/vzj2018.04.0084.

Mohammed, A.A., Cey, E.E., Hayashi, M., Callaghan, M.V., Park, Y.-J., Miller, K.L., Frey, S.K., 2021. Dual-permeability modelling of preferential flow and snowmelt partitioning in frozen soils. Vadose Zone J. 20 https://doi.org/10.1002/vzj2.20101.

Mualem, Y., 1976. A new model predicting the hydraulic conductivity of unsaturated porous media. Water Resour. Res. 12, 513–522.

Nyberg, L., Stähli, M., Mellander, P., Bishhop, K.H., 2001. Soil frost effects on soil water and runoff dynamics along a boreal forest transect: 1. Field investigations. Hydrol. Process. 15, 909–926. https://doi.org/10.1002/hyp.256.

Pittman, F., Mohammed, A., Cey, E., 2020. Effects of antecedent moisture and microporosity on infiltration and water flow in frozen soil. Hydrol. Process. 34, 795–809. https://doi.org/10.1002/hyp.13629.

Rango, A., DeWalle, D.R., 2008. Principles of Snow Hydrology. Cambridge University Press, Cambridge.

Richards, L.A., 1931. Capillary conduction of liquids through porous mediums. Physics 1 (5), 318–333. https://doi.org/10.1063/1.1745010.

Šimůnek, J., Šejna, M., van Genuchten, M.T., 1998. The HYDRUS-1D Software Package for Simulating the One-Dimensional Movement of Water, Heat, and Multiple Solutes in Variably-Saturated Media. Version 1.0. IGWMC – TPS – 70, International Ground Water Modeling Center, Colorado School of Mines, Golden, Colorado.

Stähli, M., 2017. Hydrological significance of soil frost for pre-alpine areas. J. Hydrol. 546, 90–102.

Stähli, M., Jansson, P., Lundin, L., 1999. Soil moisture redistribution and infiltration into sandy soils. Water Resour. Res. 35 (1), 95–103. https://doi.org/10.1016/j.jhydrol.2016.12.032.

Stuurop, J.C., van der Zee, S.E.A.T.M., Voss, C.I., French, H.K., 2021. Simulating water and heat transport with freezing and cryosuction in unsaturated soil. Comparing an empirical, semi-empirical and physically-based approach. Adv. Water Resour. 149.

Unold, F., Derk, L., 2017. Cryosuction – A model to describe the mechanism during ground freezing. In: PanAm Unsaturated Soils, 2017, pp. 290–299. https://doi.org/10.1061/9780784481691.029.

van Genuchten, M., 1980. A closed-form equation for predicting the hydraulic conductivity of unsaturated soils. Soil Sci. Soc. Am. J. 44 (5), 892–898. https://doi.org/10.2136/sssaj1980.03615995004400050002x.

Wang, Q., Liu, J., Wang, L., 2017. An experimental study on the effects of freeze-thaw cycles on phosphorus adsorption-desorption processes in brown soil. RSC Adv. 7, 37441–37466. https://doi.org/10.1039/C7RA05220K.

Watanabe, K., Osada, Y., 2017. Simultaneous measurement of unfrozen water content and hydraulic conductivity of partially frozen soil near 0 °C. Cold Reg. Sci. Technol. 142, 79–84.

Watanabe, K., Kito, T., Dun, S., Wu, J.Q., Greer, R.C., Flury, M., 2012. Water infiltration into a frozen soil with simultaneous melting of the frozen layer. Vadose Zone J. 12 (1) https://doi.org/10.2136/vzj2011.0188.

Watanabe, K., Kito, T., Dun, S., Wu, J.Q., Greer, R.C., Flury, M., 2013. Water infiltraiton into a frozen soil with simultaneous melting of the frozen layer. Vadose Zone Journal. https://doi.org/10.2136/vzj2011.0188.

Zhang, N., Wang, Z., 2017. Review of soil thermal conductivity and predictive models. Int. J. Therm. Sci. 117, 172–183.

Zhang, X., Sun, S.F., Xue, Y., 2007. Development and testing of a frozen soil parameterization for cold region studies. Am. Meteorol. Soc. 8, 690–701. https://doi.org/10.1175/JHM605.1.

Zhao, L., Gray, D.M., 1998. A parametric expression for estimating infiltration into frozen soils. Hydrol. Process. 11 (13), 1761–1775. https://doi.org/10.1002/(SICI)1099-1085(19971030)11:13<1761::AID-HYP604>3.0.CO;2-O.

Zhao, Y., Nishimura, T., Hill, R., Miyazaki, T., 2013. Determining hydraulic conductivity for air-filled porosity in an unsaturated frozen soil by the multistep outflow method. Vadose Zone J. 12 (1), 1–10.